Life Sciences 234 (2019) 116787

Contents lists available at ScienceDirect

Life Sciences

journal homepage: www.elsevier.com/locate/lifescie

Magnetic nanoparticles-loaded liposomes as a novel treatment agent for iron deficiency anemia: In vivo study

Mohamed M. Fathy[a], Heba M. Fahmy[a,*], Asmaa M.M. Balah[a], Faten F. Mohamed[b], Wael M. Elshemey[a,c]

[a] Biophysics Department, Faculty of Science, Cairo University, Giza 12613, Egypt
[b] Pathology Department, Faculty of Veterinary Medicine, Giza 12211, Egypt
[c] Department of Physics, Faculty of Science, Islamic University in Madinah, Saudi Arabia

ARTICLE INFO

Keywords:
Iron deficiency anemia
Magnetic nanoparticles
Liposome
Ferrous sulfate
Hematological parameters

ABSTRACT

Iron deficiency anemia (IDA) is a major worldwide public health problem. This is due to its prevalence among infants, children, adolescents, pregnant and reproductive age women. Ferrous sulfate ($FeSO_4$) is the first line therapy for iron IDA. Unfortunately, it is reported that $FeSO_4$ suffers from low absorption rate in the body and itself exhibits severe side effects. Herein, iron oxide magnetic nanoparticles-loaded liposomes (LMNPs) are prepared, characterized and evaluated as a treatment regimen for IDA in Wistar rats (as an animal model). Iron oxide magnetic nanoparticles (MNPs) are prepared and loaded into liposomes using the thin film hydration method. The size of the prepared formulations is in the range 10–100 nm, thus it can avoid the reticular endothelial system (RES), and increased their blood circulation time. For in vivo assessment, thirty-five Wistar rats are divided into 5 groups (n = 7): negative control group, positive control group, and three groups treated with different iron formulations ($FeSO_4$, MNPs and LMNPs). Anemia is induced in the anemic groups by the bleeding method and then treatment started with different iron compounds administrated orally for 13 days. Hematological parameters are followed up during the treatment period. Results indicate that, in the LMNPs group, the hematological parameters turn to normal values and the histopathological structures of the liver, spleen and kidney remain normal. This proves that liposome increases the bioavailability of MNPs. In conclusion, LMNPs demonstrate superiority as a therapeutic regimen for the treatment of IDA among the tested iron formulations.

1. Introduction

Anemia is one of the most challenged nutritional disorders all over the words, iron deficiency is the main cause of anemia, especially in developing countries due to the negative impact of a low iron diet on Hb synthesis [1,2]. Iron deficiency anemia (IDA) is associated with diminished quality of life, impaired physical and cognitive performance, resulting in lower resistance to infection, fatigue, fetal resorption, low productivity, and increased risk of maternal mortality. It also becomes life threatening if not restrained [3,4]. Iron is an abundant element on the earth, which is essential for all life forms, iron can be reduced to vital compounds which are necessary for all physiological functions in blood and body's organ (brain and muscle) such as aerobic metabolism, oxygen transport, energy metabolism, DNA synthesis and electron transport [5,6], 70% of total body's iron are inserted with Hb as a main component of Hb [7].

Ferrous sulfate ($FeSo_4$) was the first medication for the treatment of IDA [8]. However, $FeSo_4$ suffers from many disadvantages such as: having a low absorption rate in the body, decreased bioavailability in addition to having some gastrointestinal side effects like nausea, vomiting, diarrhea, flatulence, abdominal pain, dark colored stools and constipation [9,10]. These disadvantages lead to non-adherence in 50% of patients and failure of treatment [11,12].

Some researchers used Iron oxide magnetic nanoparticles (MNPs) as an iron source for iron deficiency anemia treatment because MNPs have a higher bioavailability than $FeSo_4$, in addition, MNPs increase iron absorption from gastrointestinal tract 1.35 times more than $FeSo_4$ which lowers the gastrointestinal side effects [13–15]. Salah and coworkers registered patent for using magnetite nanoparticles capped with vitamin c which was administrated IP or orally (without any drug carriers) as a single dose for the treatment of anemia and found that his formulation raises Hb levels to normal values in 10 days and also

* Corresponding author at: Biophysics Department, Faculty of Science, Cairo University, 12613, El Gamaa street, Giza, Egypt.
E-mail address: hfahmy@sci.cu.edu.eg (H.M. Fahmy).

https://doi.org/10.1016/j.lfs.2019.116787
Received 28 June 2019; Received in revised form 17 August 2019; Accepted 20 August 2019
Available online 21 August 2019
0024-3205/

increases the production of RBCs, in addition to increasing erythropoiesis [16].

Garces et al. used MNPs and incorporated them inside fermantus bacteria to obtain (MNPs-bacteria) as a new formulation for the IDA treatment [17]. Also, it was reported that iron oxide nanoparticles capped with multi vitamins (folic acid, vitamin B9 and vitamin c) could be used for IDA treatment [18]. Moreover, El Shemy added iron oxide nanoparticles in drinking water to be used as a supplement for IDA treatment [19]. Also, many reports investigated the bioavailability of different iron formulations [20,21]. Finally, Kheiri et al. studied the effect of oral iron oxide on serum iron (Fe) and total iron binding capacity (TIBC) and compare the results with those of $FeSo_4$ [22].

Unfortunately, MNPs aggregation in the biological system affects their colloidal stability and cause toxicity, this can be overcome by coating their surface [23,13]. Coating MNPs with different materials protects them from the body immune system, increasing their stability in the body fluid, to overcome acute agglomeration of MNPs and obtain biocompatible MNPs [24–26].

Liposomes are synthesized from natural compounds that make them biocompatible and biodegradable. Liposomal biocompatibility is the main reason for drug protection against enzymatic degradation and decreasing their toxicity. Liposome increases the stability of therapeutic drug, enabling the drug to stay much longer time in the blood circulation and enhances the blood bio distribution. Liposome is considered as the most adequate drug delivery system because it leads to increasing drug efficacy, the ability of drug targeting by active or passive targeting, controlled release of the drug at a predetermined rate with avoiding the immune response stimulated by oral drug delivery [27,28]. The aim of this work is to prepare LMNPs that enhance iron absorption and to solve noncompliance problems of iron treatment. And evaluate the potency of the prepared LMNPs as a treatment regimen for iron deficiency anemia.

2. Materials and methods

2.1. Materials

Iron (II) (99.99%) trace metals basis, Iron (III) 98% purified lumps, L- Ascorbic Acid 99% crystalline, Soybean (mixture of phospholipid), Cholesterol from lanolin > 99.0% (GC), Ammonium hydroxide, chloroform solution (HPLC grade) were purchased from Sigma Aldrich, Germany.

2.2. Methods

2.2.1. Preparation of iron oxide magnetic nanoparticles (MNPs)

Firstly, the iron metal base was weighted and dissolved in 40 ml distilled H_2O to make an aqueous sample of Fe (III) and Fe (II) salts in a molar ratio of 2:1. The solution was sitting for 15 min at stirring for complete dissolution. After that, 2 ml of ascorbic acid (0.1 g/ml) was weighed and dissolved in 2 ml distilled H_2O, then added to the solution to obtain a sample mixture of MNPs and ascorbic acid at molar ratio 1:1. Before adding ascorbic acid and the reaction temperature was raised to 40 °C. After adding all of the ascorbic acid, the mixture color changed to yellow color. Following this step, the reaction temperature was raised to 85 °C. Then, 5 ml of ammonium hydroxide was added to the solution, the solution color was converted to black. The solution was then left for 1 h with continuous stirring. Finally, the precipitate was washed several times with saline to remove excess ammonia and left to dry.

2.2.2. Preparation of iron oxide magnetic nanoparticles-loaded liposome (LMNPs)

LMNPs were prepared according to the method of [29], with slight modification (by adding cholesterol to soybean phosphatidylcholine) to increase rigidity of the lipid bilayer and to decrease its fluidity [30]. Soybean phospholipid and cholesterol were at molar ratio 2:1 respectively. The mixture was then dissolved it in 5 ml of chloroform (organic solvent) in a round bottom flask to reach a final concentration of 20 mmol/l (To obtain a lipid concentration of 20 mmol/l). The organic solvent was evaporated on a rotary evaporator at 40 °C then the flask placed under vacuum pump to form a thin lipid film completely dried from organic solvent.

The lipid film was hydrated with the appropriate amount of MNPs solution to encapsulate them inside the lipid vesicle [31]. To prevent the aggregation and the deposition of larger particles, the MNPs must be dissolved in 10 ml saline (as the hydration medium) 24 h before the experiment, with 10 min sonication to ensure complete homogeneity.

The final obtained solution was applied to bath sonicator for 1 h to obtain unilamellar vesicles of magneto liposome. Sonication was used to provide sonic energy which disrupts the large multilamellar vesicles to small unilamellar vesicles with diameters in the range of 15–50 nm. The non-loaded magnetic nanoparticles are removed by using centrifugation [31]. The concentrations of non-loaded (unencapsulated MNPs in the supernatant) MNPs were calculated from the calibration curve that was performed at 220 nm by UV–visible spectrophotometer (Jenway 6405, Barloworld Scientific, Essex, UK) [32].

2.2.3. Characterization of the prepared nano-formulations

Transmission electron microscope (TEM) technique was used to visualize the morphology and the size distribution of the nanoparticles [33].

For MNPs, one drop of the sample was applied to a carbon grid coated with copper and left to dry for 5 min at room temperature, a filter paper was then used to remove the all excess samples. For magneto liposome, the same procedure was used, but with slight modification: after the sample drop has been dried and before imaging, a contrast agent (phosphotungestic acid, PTA) was used as a negative staining, thus protecting the sample structure from being damaged by the electron beam. This helped to obtain an accurate image of the liposome structure [29].

DLS measures the mean size and distribution of particles in liquid suspension, which is expressed by the velocity of Brownian motion, resulting from the collision of particles to each other. Brownian motion velocity can be recognized by translational diffusion coefficient D [34]. Zeta potential is used to measure the electrical charge of particle surface [35]. Surface potential and size distribution of MNPs and LMNPs were determined at room temperature using the Zeta Potential/Particle Seizer (NICOMP TM 380 ZLS, USA).

2.2.4. In vivo experiments

2.2.4.1. Animals used. Thirty-five adult female Wistar rats weighing (100–120 g) were obtained from a local supplier, Cairo, Egypt. These animals were placed (housed) in clear plastic cages which bedspread with sawdust and were placed in room streaked with a suitable environment (22 ± 3 °C and 50% ± 10% relative humidity) with a 12-hour dark/light cycle. Sawdust was renewed every two days. Rats were provided with sufficient feeding and water ad-libitum.

Experimental procedures were achieved in conformation with the principles of laboratory animal care and approved by the institutional animal care and use committee Cairo University, Egypt (Registration no.: CUIS 75 17).

2.2.4.2. Experimental design. All experimental animals were adapted one week before the beginning of the experiment. After adaptation, blood samples from all animals were collected in EDTA tubes to examine the hematological parameters to be sure that initially the experimental animals were not anemic.

Rats were divided among the experimental groups randomly (7 rats in each group). The first group was the negative control group. The remaining 28 rats were used as iron deficiency- induced model. The bleeding method was used to induce anemia in rats [16]. After anemia

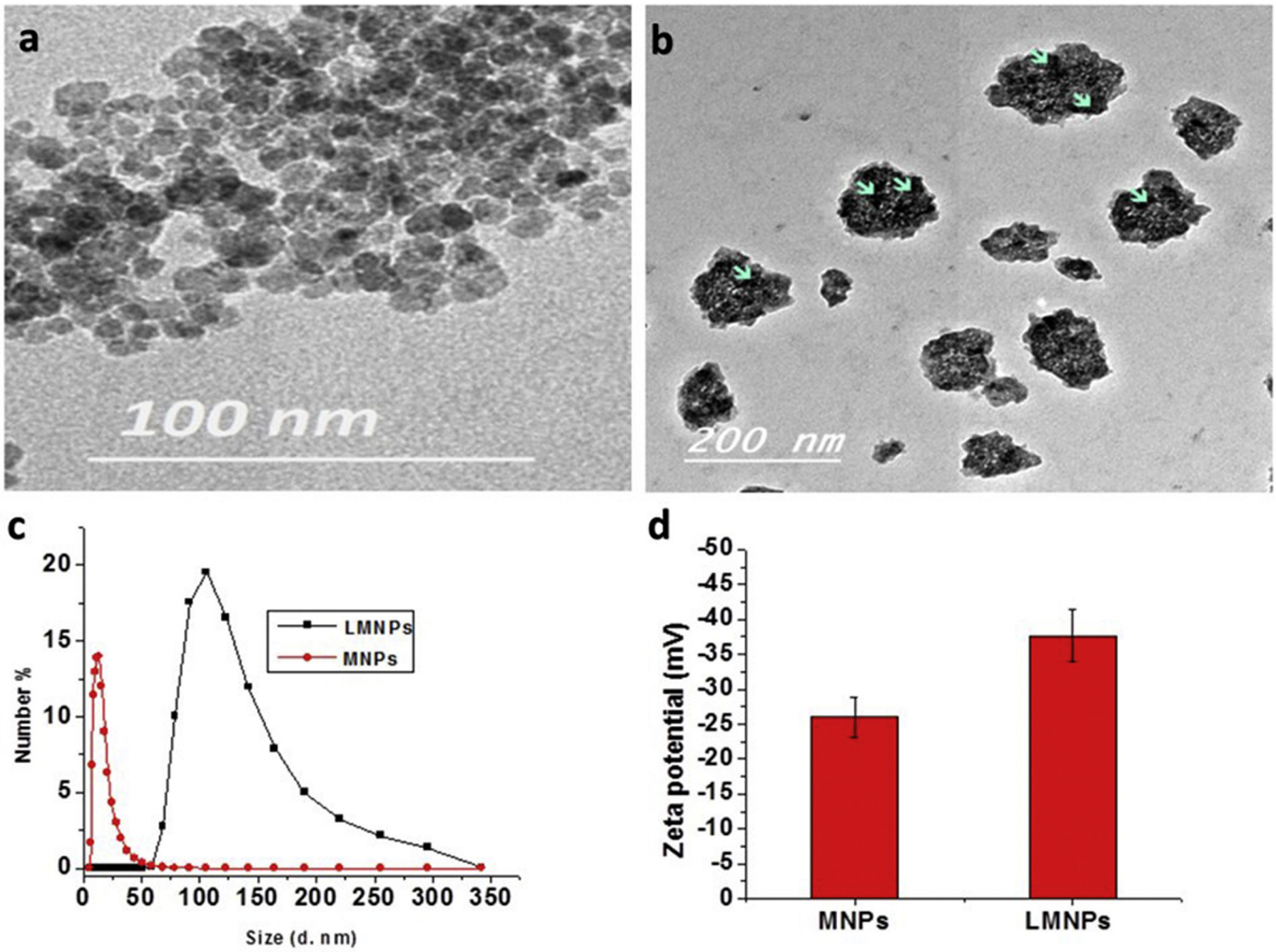

Fig. 1. a) TEM micrograph of magnetic nanoparticles (MNPs), b) TEM micrograph of liposome magnetic nanoparticles (LMNPs), c) Dynamic light scattering distribution of MNPs and LMNPs. d) The zeta potential of MNPs and the zeta potential distribution of LMNPs.

induction, blood samples were collected to confirm the success of the animal model. Anemic rats were then randomly divided into 4 groups: (1) The positive control group (received no treatment), (2) The $FeSO_4$ group: which is an anemic group treated with ferrous sulfate as an anemic reference drug, (3) MNPs– treated group: which is an anemic group treated with MNPs and (4) the last group, LMNPs group: which is an anemic group treated with MNPs encapsulated inside liposome.

2.2.4.3. Anemia induction. Anemia was induced in the anemic groups by the bleeding method. Briefly, 1 ml blood was withdrawn daily for five successive days from the rat ocular eye vein. On the fifth day of anemia induction, blood samples were collected from all the experimental groups to examine the hematological parameters. Anemia induction was considered successful when the hemoglobin (Hb) levels became < 9.0 g/dl [36].

2.2.4.4. Treatment design. Treatment period started directly the day after anemia induction and continued for 13 days. Rats in the three-treatment groups were treated with three different iron compounds ($FeSO_4$, MNPs and LMNPs) but with the same dose of iron (12 mg/kg of body weight) according to [37]. The treatments were given orally, all the formulations were daily freshly prepared, and the intra-gastric administration was performed daily at 10 am. Rats body weights were monitored daily along the experiment period.

2.2.4.5. Blood collection. Blood samples were withdrawn from the rat ocular vein using a capillary tube, then blood sample were collected in EDTA tubes (as anti-coagulant) to examine hematological parameters.

2.2.4.6. Determination of hematological parameters. Before the beginning of the experiment hematological parameters were measured in all rats and their values were statistically non-significant between all the experimental groups ($P > 0.05$). Hematological parameters were measured in rats in all groups during the experimental periods (before anemia induction, first day of treatment, day 3 post treatment, day 7 post treatment, day 10 post treatment and day 13 post treatment. The hematological parameters that were measured were hemoglobin (Hb), red blood cell (RBC) and white blood cell (WBC) [Total leucocyte count (TLC)]. They were measured by automated differential blood cell counter (Mind ray 2800, China).

2.2.4.7. Blood smear preparation. Blood samples which were collected for hematological tests, were also used in blood smear preparation. Blood films were stained with alkaline methylene blue and with Giemsa's stain. They were viewed by Labomed USA microscope, projected at 40× magnification.

2.2.4.8. Histopathological examination. At the end of the experiment, Liver, spleen and kidney were collected from rats in all groups, they were then settled in 10% formalin. Alcohol gradient solutions were

used for samples dehydration and xylene for clearance, finally samples were paraffin- embedded. Hematoxylin and Eosin stain were used for slides' samples staining. A light microscope was used for sample examination with a ×400 magnification according to the method of [38].

2.2.5. Statistical analysis

The data were manifested as mean ± standard error of the mean (S.E.M.). Data analysis was performed by one-way ANOVA, followed by a post hock test, to compare between the different experimental groups, the least significant difference (LSD) test was used. Data were analyzed statistically with the statistical package for the social sciences (SPSS) version 22. The values were considered statistically significant if ($p < 0.05$).

3. Results and discussion

3.1. Transmission electron microscope (TEM)

TEM technique was used to investigate the shape and size of the prepared nano-formulations. The TEM micrograph of the prepared MNPs showed that the formed nanoparticles were well dispersed, with spherical morphology, and homogenous diameter size distribution of about 7 nm (Fig. 1.a). The prepared LMNPs were spherical in shape and they have low aggregations as shown in Fig. 1.b. Also, MNPs were observed in the core of the liposomal assembly (the darker color parts inside liposomes, indicated by arrows). From these results, it is shown that MNPs could be entrapped in the hydrophilic part of the liposomal system.

3.2. Dynamic light scattering (DLS)

DLS is a technique which is being used to assess the hydrodynamic diameter and size distribution of the prepared nanoparticles. It was reported that the hydrodynamic size of MNPs affects their distribution, pharmacodynamics, blood clearance pharmacokinetics and determine their stability [39]. The hydrodynamic sizes of the prepared formulas were 10 ± 2.6 nm and 125 ± 5.8 nm for MNPs and LMNPs, respectively, as shown in (Fig. 1.c).

It was found that, smaller nanoparticles with diameters < 10 nm are filtrated from the body by the kidney through renal clearance [39,40]. On the other hand, larger sized nanoparticles (200 nm) have higher accumulated through spleen sinusoids, that results in small blood half-life time [40–42]. In contrast, nanoparticles with diameters around 100 nm, have targeting ability to more organs with effective distribution and can avoid reticuloendothelial system (RES) and thus, increasing their circulation life time [40,43–45].Hence, in this study LMNPs were prepared in nano-sized range (around 100 nm).

DLS provides information about the polydispersity of the sample via the Polydispersity Index (PDI). PDI usually ranges from 0.05 to 0.7, increasing PDI value indicates a wide nanoparticle distribution (PDI > 0.5indicates an inhomogeneous particle size distribution), which results in their multi-stage clearance so that larger nanoparticles have lower blood half- life time than smaller ones [46,47]. The polydispersity index (PDI) distribution of MNPs was 0.229 and that for LMNPs was 0.473 indicating homogeneous size distributions of the prepared nano-formulations.

3.3. Zeta potential

Zeta potential is a technique for measuring the electrical charge of the particle surfaces that determine their stability in the colloidal system. Pharmacokinetics of nonmaterial in blood circulation depends on their zeta potential, because the surface charge of nanoparticles may alter their electrostatic interaction with surrounding proteins [47–49]. The average zeta potential of prepared MNPs was −25 ± 5.65 mV (Fig. 1.d), this negative charge is attributed to the ascorbic acid hydroxyl group that is found on MNPs surface [50–52]. After loading of MNPs within liposome, the average zeta potential of LMNPs was −37 ± 5.16 mV, this increase in the negativity is due to the negative charge of the phosphate end group of liposomes [53]. Also, cholesterol content through liposomal bilayer increase negativity as the hydroxyl group of cholesterol-polar head group combines with choline in polar regions in the phospholipid to produce the type of dipole tropism that increase the negative charge on the liposome surface [54]. It was reported that cholesterol increases the stability of the liposome in biological fluid like in blood plasma through the decreasing of the membrane fluidity and the reduction of the membrane permeability [29,55].

It was found that positively charged nanoparticles have the circulation half-life time of about (1–2 min) while blood half-life of negative ones was (40–50 min) [56,57]. As positive nanoparticles are taken faster with macrophage due to the electrostatic interaction that occur between the negative charge of the phosphate end group on macrophage surface and the positive charge on the nanoparticles surface while the negative one has low opsonization rate due to decreasing macrophage recognition and the uptake for negative nanoparticles due to electrostatic repulsion [58]. Moreover, in previous studies, it was found that, MNPs with positive surface charge have higher affinity for protein adsorption on their surface and hence macrophage binding [56,57,59,60].

In our study, loading of MNPs into liposome increases their stability and enhance their surface properties, as they can evade RES and avoid opsonization [61–63].

3.4. Hematological parameters

During the treatment period, different hematological parameters [Hemoglobin (HB), Red blood cell (RBC) and Total leucocyte count (TLC).] were measured to assess the effectiveness of different iron formulations in the improvement of iron deficiency anemia. These parameters are the main diagnostic tool for IDA [64].

3.4.1. Hb values

Hemoglobin is the main protein in RBCs that is responsible for oxygen transport to different tissues and has a main role in many metabolic processes [65]. So, Hb values were measured to confirm the existence of anemia, and to follow up the recovery during the treatment period [66].

The Hb results showed that before starting the experiment all treated groups (LMNPs, MNPs and $FeSO_4$) had normal Hb values [14.07, 13.25 and 12.98 (g/dl)], respectively (Fig. 2.a). After anemia induction, by withdrawing 1 ml of blood each day for four successive days [16], Hb values of all groups dropped to anemic range values with respect to the first day of the experiment. After anemia induction, Hb values were significant compared to the –ve control group (normal group, 13.4 g/dl). Hb values of +ve control, $FeSO_4$, MNPs and LMNPs groups after anemia induction were 7.05, 7.15, 7 and 7.3 g/dl, respectively. This verified the induction of anemia in different experimental groups. Three days after treatment, the Hb values of LMNPs group (9.9 g/dl) and $FeSO_4$ (9.58 g/dl) group significantly increased compared with the +ve control group. Meanwhile, the MNPs group revealed non-significant increasing for the Hb levels compared with the positive control group.

Five days after treatment, results showed a persisting improvement for the Hb values of LMNPs and $FeSO_4$ groups (10.63 g/dl and 10.3 g/dl, respectively) compared with the MNPs and +ve control groups (9.25 and 8.1 (g/dl)). Interestingly, LMNPs group showed a noteworthy improvement for Hb values over $FeSO_4$ group.

Ten days after treatment, further improvement in Hb values for LMNPs (11.88 g/dl) and $FeSO_4$ groups (11.13 g/dl) was reported and the values of both groups were significantly different from the +ve control group and the MNPs group. MNPs group showed a significant

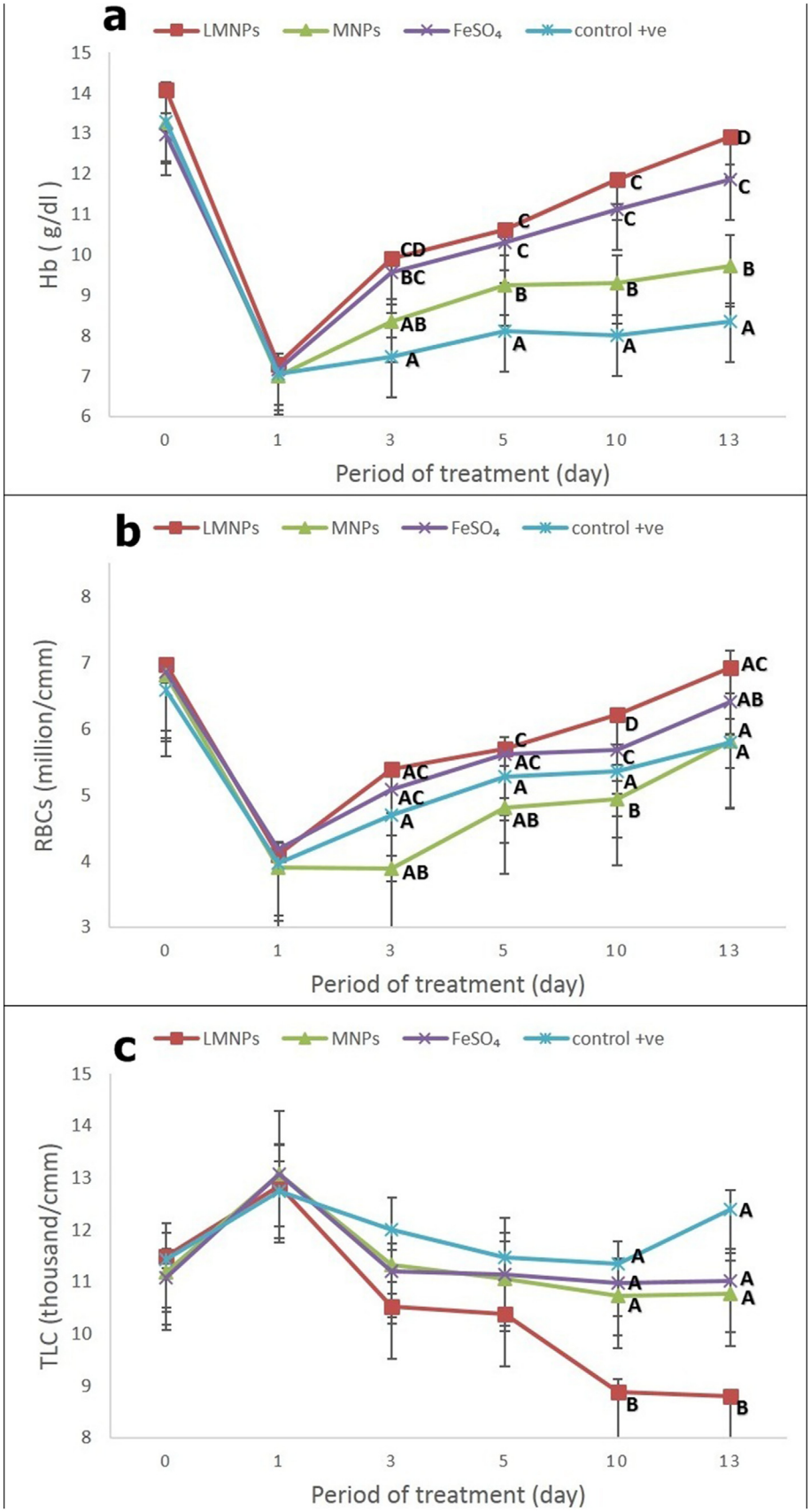

Fig. 2. a) The increase in Hb concentration during the treatment period for different groups (MNPs, LMNPs, FeSo4 and +ve control), b) the increase in the RBCs count during the treatment period for different groups (MNPs, LMNPs, FeSo4 and +ve control), c) the increasing in the TLC count during the treatment period for different groups (MNPs, LMNPs, FeSo4 and +ve control). (Number per group = seven rats). Error bars represent the variability of the measured data on the graph, reflect the precision of the measurements and indicate the error percentage of the reported data.

increase in the Hb value compared with the +ve control group.

Finally, thirteen days post treatment, LMNPs group had the highest Hb value (12.93 g/dl) which was significantly different from $FeSO_4$ (11.85 g/dl), MNPs (9.73 g/dl) and +ve control groups (8.35 g/dl).

Some researchers used MNPs as an iron source for iron deficiency anemia treatment because MNPs had higher bioavailability than $FeSO_4$ and increase the iron absorption from the gastrointestinal tract (1.35 times than $FeSO_4$) which improved the treatment efficiency, decrease the used doses of drugs, decrease gastrointestinal side effects and enabled the patient to continue the treatment period [13–15,67,68]. On the other hand, MNPs aggregation in biological system affected their colloidal stability and could cause toxicity. In a previous study, it was reported that MNPs showed a non-remarkable increase in Hb values and the animals treated with MNPs were still anemic [69]. Consequently, the biocompatibility, the pharmacokinetics and the pharmacodynamics of MNPs could be improved by coating their surfaces with different bio-capping materials [13,70–72].

Biocompatibility was reported as the main reason for drug protection against enzymatic degradation which, consequently, increased the stability of therapeutic drugs, enabled them to stay much longer time in blood circulation and enhanced their blood distribution [73,74].

Results proved the superiority of LMNPs as therapeutic regimen for the treatment of IDA and returning the Hb concentrations to nearly their normal levels over the other iron formulations ($FeSO_4$ and MNPs). The findings of the present study were in line with those of previous studies which confirmed that naturally synthesized liposomal carrier increased the bioavailability of different drug molecules resulting in higher bioavailability of LMNPs over $FeSO_4$ and MNPs [65,66,75].

Ferrous iron salts were the first line therapy for IDA as oral iron treatment, and $FeSO_4$ were the most popular oral iron therapy prescribed for anemic patients [76,77]. The main trouble with these therapies were their gastrointestinal side effects that formed free radicals proliferation of redox reaction in gut lumen at mucosal surface which lead to inflammation resulting in decreasing the absorbance of molecules from gastric wall, abdominal pain and constipation [78–80]. These effects lead to non-adherence in 50% of patients, resulting the failure of treatment [11,12,81,82].

3.4.2. Number of RBCs

RBCs productions were affected by Hb concentration. Decreasing the amount of iron in the body (iron deficiency anemia) leads to decreasing Hb formation, as a result, RBCs production also decreases [83].

In the present work, it was observed that, after induction of anemia, the RBCs count significantly decreased for all groups (4.1, 3.9 and 4.18 (million/cmm) for LMNPs, MNPs and $FeSO_4$, respectively) with respect to the first day of the experiment (6.97, 6.81 and 6.85 (million/cmm) for LMNPs, MNPs and $FeSO_4$, respectively) (Fig. 2.b).

Three days after the start of the treatment, the RBCs number for LMNPs (5.39 million/cmm), MNPs (3.89 million/cmm), and $FeSO_4$ (5.08 million/cmm) showed no obvious improvement in their values [they were statistically non-significant compared to the +ve control group (4.7 million/cmm)]. The RBCs number for LMNPs and $FeSO_4$ groups were significant different from the MNPs group. Five days after the treatment, the improvement in RBCs count for LMNPs group (5.96 million/cmm) increased significantly compared with the +ve control group (5.27 million/cmm), and MNPs group (4.8 million/cmm). Ten days after the treatment, the results showed a further significant increase in the RBCs count for LMNPs group (6.21 million/cmm) compared to the +ve control group (5.36 million/cmm), $FeSO_4$ group (5.68 million/cmm) and MNPs group (4.93 million/cmm). $FeSO_4$ group also showed significant increase in their RBCs count, compared to the +ve control group and MNPs group. MNPs (4.93 million/cmm) group recorded significantly lower RBC count than the +ve control group (5.36 million/cmm). Thirteen days after treatment, LMNPs (6.92 million/cmm), was the only group that revealed remarkable increase in their RBCs count over the +ve control group (5.79 million/cmm), MNPs group (5.8 million/cmm), and $FeSO_4$ group (6.4 million/cmm). These results, which were consistent with Hb values assessment, proved that treating animals with LMNPs success in the refinement of anemia symptoms compared to other formulations, like in [66].

Iron compounds have toxic effects on RBCs, which appeared in MNPs-treated group. RBCs number of LMNPs group did not decrease like in MNPs group, which meant that liposomes protect the body from iron toxicity. The decrease in RBCs count in MNPs group might be attributed to the hemolysis effect of uncoated MNPs on RBCs that was reported in some previous studies. [84] reported that uncoated MNPs showed severe dose-dependent hemolysis when these nanoparticles were incubated in mouse erythrocyte suspension for 4 h at 37 °C. They added that rapid hemolysis or capillary blockage might occur due to aggregation of uncoated MNPs when the dose reached 2.5 mg/kg or above, which might lead to animal death.

Coating of MNPs was required in biological applications to protect them from aggregation in blood plasma due to high surface energy of MNPs, which lead to macrophage uptake by the reticulo-endothelial system. Thus, coating could minimize their surface energy and verify their stabilization in biological systems [85,86].

Liposome consisted of lipid molecule (the main component of cell membrane). This made them biocompatible, biodegradable and lowered their cytotoxicity. Liposomes were used in several biomedical applications due to their ability to encapsulate both hydrophilic and hydrophobic drugs. They could also control drug size between 20 nm and 1 μm and had the ability of surface manipulation with diverse methods [87,88].

When MNPs were encapsulated in liposome, the inner bilayer surface bound tightly with MNPs by chemo sorption forces making LMNPs impervious to osmotic pressure [89]. Liposomes enhanced the stability of MNPs because of enhanced permeability, retention effect (EPR), the decrease in the tendency of MNPs to aggregate and decrease the hemolytic potential of MNPs on RBCs [90–93]. Liposomes do not release their content when they enter the blood stream and remain stable [94]. Liposomes preserve their spherical shapes if incubated with plasma constituents [95].

In Xia & Xu study, they found that when $FeSO_4$ were coated with liposomes they demonstrated similar bioavailability to that of $FeSO_4$ but, liposomes provided the additional benefit that it protected the iron from interacting with the surrounding food in the gastrointestinal tract and prevented any undesirable reaction that might occur due to iron therapy [54].

3.4.3. Total leucocyte count (TLC)

The results of total leucocyte count (TLC) of different groups during the experimental period are shown in Fig. 2.c. It could be noticed that the only significant improvement (decrease) in the TLC compared to +ve control was reported for the LMNPs group at the 10th and 13th days of treatment. At 10th day TLC values were (11.35, 11.03, 10.78 and 8.88 thousand/cmm) for (+ve control, $FeSO_4$, MNPs and LMNPs, respectively), at 13th day TLC values were (12.4, 11.03, 10.78 and 8.8 thousand/cmm) for (+ve control, $FeSO_4$, MNPs and LMNPs, respectively). The TLC elevation after the induction of anemia gave an indication on the activation of the body immune system. This activation was probably because of the use of the bleeding method for induction of anemia that was previously proved to cause inflammation in the rats' eyes [64,96].

The obtained results could be attributed to that iron compounds in $FeSO_4$ and MNPs groups caused inflammation, which resulted from free radicals' diffusion due to redox reactions that occurred in the gastrointestinal tract. These inflammations affect the immunological function, like in the work of [69], who studied the effect of Titanium dioxide nanoparticles (TiO_2 NPs) on hematological parameters. The present study showed an increase in TLC indicating immune defense activation [78–80]. In the LMNPs group, the immunological function was not affected.

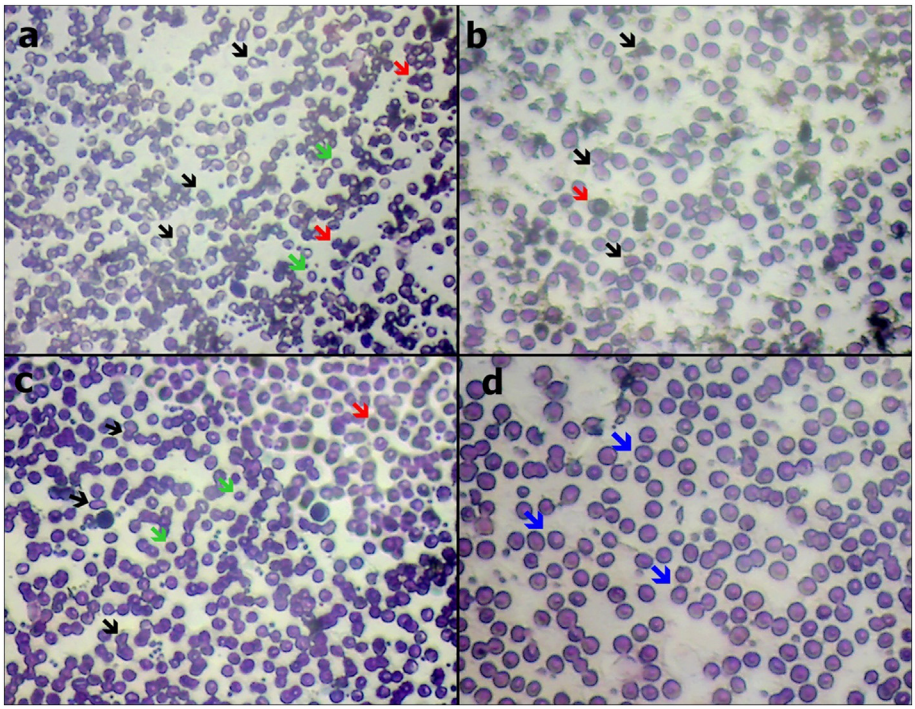

Fig. 3. a, b, c and d: Blood films examined under light microscope, Labomed USA (magnification 40×) of (a) the control +ve group and (b, c & d) treated groups (MNPs, FeSO4 and LMNPs, respectively) after 13 days of treatment. (Black arrows for poikilocytosis, red arrows for hypochromasia, green arrows for anisocytosis and blue arrows for normal red cells). The +ve control group (a) shows schistocytes, severe poikilocytosis, microcytes and hypochromasia, indicated by arrows. The $FeSO_4$ group (b) shows poikilocytosis, hypochromasia and little schistocytes, indicated by arrows. The MNPs group (c) illustrates severe poikilocytosis, microcytes with numerous schistocytes, indicated by arrows. The LMNPs group (d) shows normal shaped RBCs with little poikilocytic cells, indicated by arrows. (Number per group = seven rats). (Scale bar: μm). (For interpretation of the references to color in this figure legend, the reader is referred to the web version of this article.)

3.5. Blood smear

The morphology of RBCs in a blood film was considered as a main criterion for characterizing anemic rats. In anemic +ve control (untreated) group, rats' blood films showed changes in the size and shape of RBCs. Poikilocytosis (abnormal RBCs shapes such as tear-dropped shape, sickle shape, elongated shape and irregularly contracted), anisocytosis (varied RBCs size) due to presence of microcytes, hypochromasia (paler RBCs than normal), spherocytosis (sphere-shaped cell) and schistocytes (jagged cells) were all present (Fig. 3.a).

RBCs normal shapes were biconcave disk shaped with pallor area in the center [97]. Poikilocytosis, hypochromasia, spherocytosis and schistocytes appearance gave indication on a degree of RBCs membrane damage due to hemolysis effect (hemolytic anemia) and RBCs membrane abnormalities. [98,99].

After 13 days of treatment, the $FeSO_4$-treated group showed RBCs' membrane abnormalities in their blood films like poikilocytosis, anisocytosis, hypochromasia and schistocutes (Fig. 3.b). There are marked poikilocytosis in MNPs' films and the normal RBCs-shaped cells nearly disappeared like in anemic rats' films. This reflected acute hemolysis and also confirmed the previously discussed results of the hematological parameters. Also, poikilocytosis, anisocytosis, hypochromasia and schistocutes appeared in MNPs' film (Fig. 3.c).

In LMNPs group, the blood film demonstrated that the majority of RBCs had normal shaped cells (biconcave disk shape with pallor area in the center) with little poikilocytosis (Fig. 3.d). This added more evidence of the protective role of LMNPs.

3.6. Histopathological alterations

The histopathological examination was performed to study the effect of different iron formulations ($FeSo_4$, MNPs and LMNPs) on the spleen, liver and kidney.

3.6.1. Spleen

The microscopic examination of –ve control (normal) group revealed normal histological structure of red pulp with very few numbers of erythroid cells and megakaryocytes associated with fine hemosiderin pigment deposition (Fig. 4.a). The splenic red pulp of the +ve control group showed increased extramedullary hematopoiesis, the lesion was characterized by infiltration of red pulp by many immature erythroid, myeloid elements in red pulp as well as the appearance of megakaryocytes (Fig. 4.b & c). The splenic lesions that represented hematopoiesis were declined in $FeSO_4$-treated group with minimal number of erythroid and myeloid elements and individual number of megakaryocytes that were detected in splenic red pulp (Fig. 4.d). The microscopic examination of MNPs-treated group showed the minimal erythroid number with the deposition of hemosiderin pigment free and in macrophages, but the number of megakaryocytes was relatively increased compared with $FeSO_4$-treated group (Fig. 4.e). The relative increased megakaryocytes number with hemosiderin deposition assumed to be related to RBCs destruction induced by the toxic effect of MNPs on RBCs. Valberg & Butler reported that in vitro RBCs hemolysis occurred when IONP was added to RBCs [100], also Feng et al. reported that IONPs induced severe dose-dependent hemolysis when IONPs were incubated with mouse erythrocyte suspension for 4 h at 37 °C [84]. The splenic red pulp lesions of LMNPs group were extremely scarce represented by fine hemosiderin pigment deposition (Fig. 4.f). The white pulp of –ve control (normal) group showed normal histological structure of lymphoid follicles (Fig. 5.a) while the splenic lesions of the +ve control group showed mild lymphocytic depletion (Fig. 5.b). The lesions comprising lymphoid follicle of $FeSO_4$-treated group were severe and characterized by necrosis and lymphocytolysis with the appearance of tangible body macrophages (Fig. 5.c). The normal structure of lymphoid follicles was observed in MNPs (Fig. 5.d) and LMNPs-treated groups with no detectable lesions, the appearance of splenic lesions (necrosis) in $FeSO_4$ group confirms the toxic action of $FeSO_4$ on the spleen, while in MNPs and LMNPs-treated groups, there was no recognized toxicity on splenic tissue.

3.6.2. Liver

Concerning liver, the microscopic examination of –ve control (normal) group revealed normal histological structure of hepatocytes and hepatic parenchyma. Multi focal sinusoidal leucocytosis and dilatation were observed in the +ve control group with focal necrosis of hepatocytes (Fig. 6.a). Hepatic lesions in $FeSO_4$-treated group were

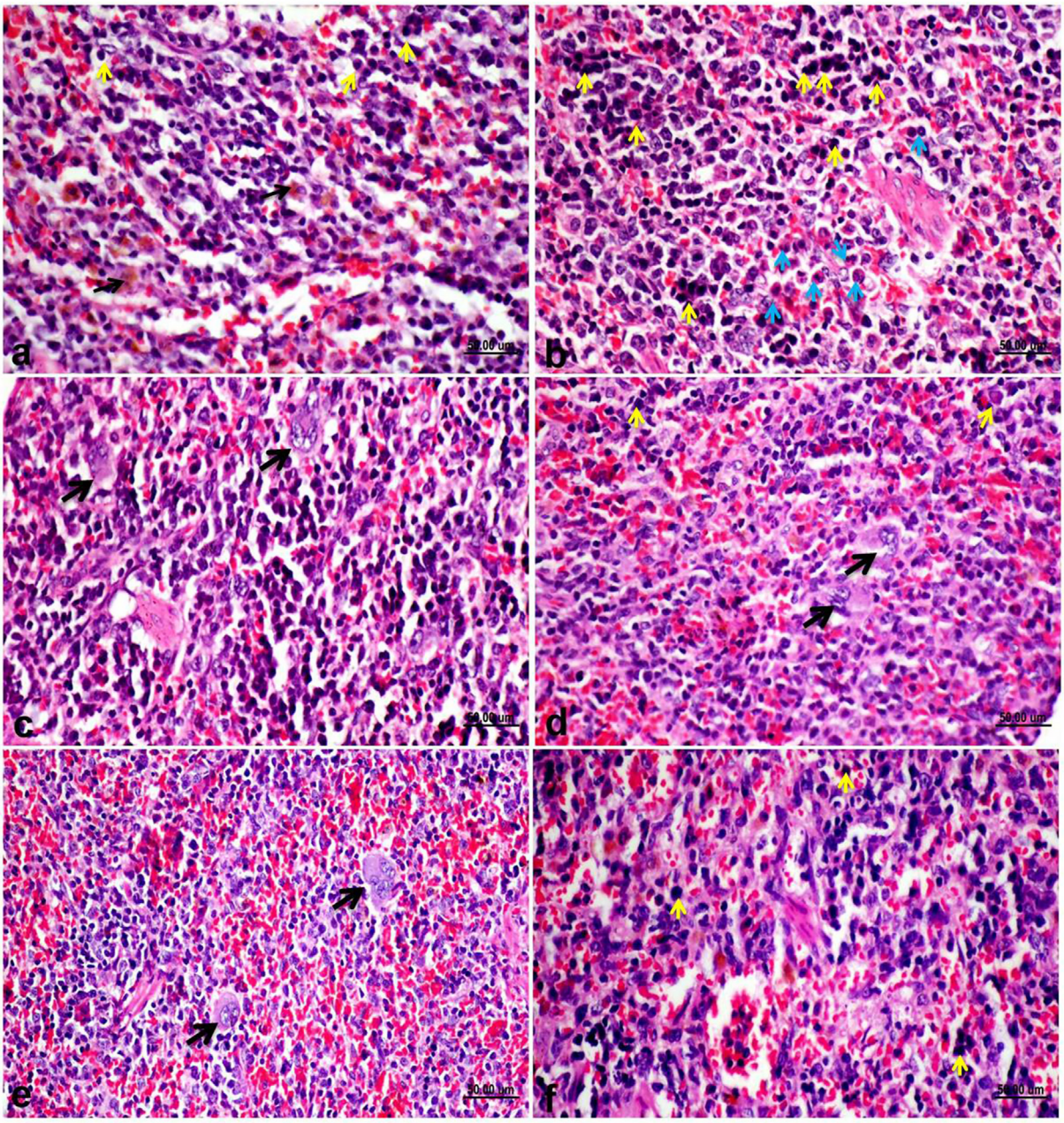

Fig. 4. Histological section of the spleen (H&E, X600). (yellow arrows for erythriod precursors, blue arrows for myeloid precursors, thick black arrows for megakaryocytes and thin black arrows for hemosiderin) (a) –ve control untreated group showing scarce erythroid precursors with fine hemosiderin pigment deposition. (b & c) +ve control group showing infiltration of red pulp by erythroid and myeloid elements (b) and megakaryocytes (c). (d) FeSO4-treated group showing a low number of erythroid elements with the appearance of megakaryocytes. (e) MNPs-treated group showing few erythroid cells with megakaryocytosis. (f) LMNPs-treated group showing scarce erythroid elements infiltrating the red pulp and fine hemosiderin deposition. (Number per group = seven rats). (Scale bar: 50 μm). (For interpretation of the references to color in this figure legend, the reader is referred to the web version of this article.)

more severe than in the +ve control group. There was a mononuclear cell infiltration in the portal area with fine hemosiderin pigment deposition in individual macrophages with mild sinusoidal leucocytosis and focal hepatocellular necrosis (Fig. 6.b). The hepatic lesions in MNPs-treated group was minimal compared with $FeSO_4$-treated one also Kupffer cell activation was observed in MNPs group (Fig. 6.c). The liver of LMNPs-treated group showed normal hepatic histological structure with no detectable hepatic lesions (Fig. 6.d), the histopathological examination of liver clarifies the toxic effect of $FeSO_4$ group on the liver which was not detected in the remaining treated groups (MNPs & LMNPs).

3.6.3. Kidneys

The kidney of the normal group showed normal histological structure of renal cortex and medulla (Fig. 7.a). Renal lesions in the +ve control group were detected in renal tubules and were characterized by vacuolization and necrosis of tubular epithelium (Fig. 7.b), the lesions were considered mild in their severity. The vacuolization of tubular epithelium was minimal in $FeSO_4$ and MNPs-treated groups (Fig. 7.c & d). The normal histological structure of renal tubules was observed in the LMNPs-treated group.

The results of the present study indicated that LMNPs have therapeutic potential for anemia in experimentally induced anemic animal model with less toxic effect on parenchymatous organs compared with

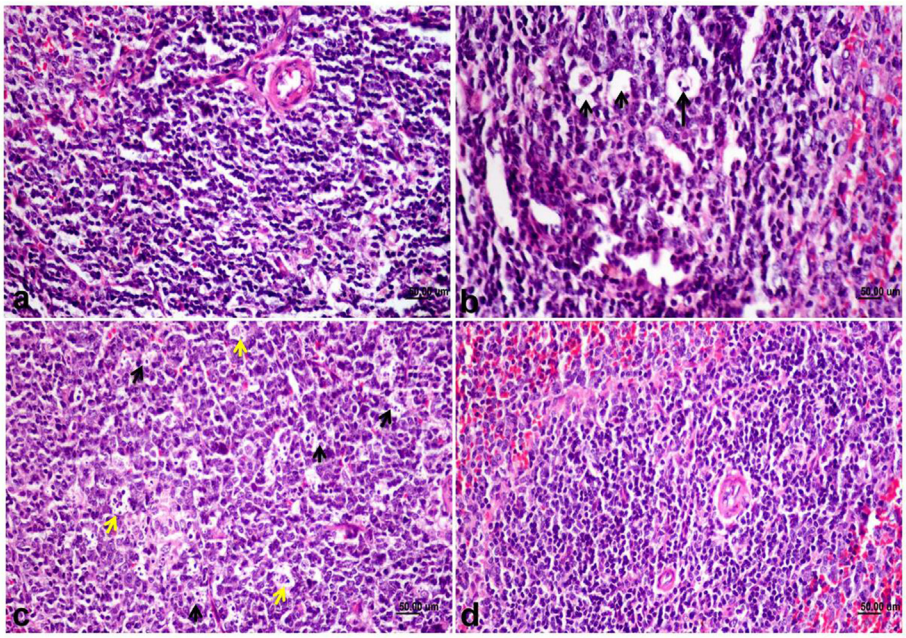

Fig. 5. Histological section of spleen (H&E, X200). (a) –ve control untreated group showing normal histological structure of lymphoid follicles. (b) +ve control group showing lymphocytolysis (long arrow) and lymphocytic depletion (short arrows comprising the follicle. (c) FeSO4-treated group showing massive necrosis of lymphoid elements (short black arrows) with the appearance of tangible body macrophages (yellow arrows). d) MNPs-treated group showing normal histological structure of lymphoid follicles. (Number per group = seven rats). (Scale bar: 50 μm). (For interpretation of the references to color in this figure legend, the reader is referred to the web version of this article.)

the commercial therapeutic drugs.

4. Conclusion

In the present work, magnetic nanoparticles capped with vitamin c and encapsulated inside liposome (soybean + cholesterol) were prepared successfully. The present results proved that LMNPs had a greater efficiency in treating IDA compared with the two other tested formulations (MNPs and $FeSO_4$) as they were able to return the hematological parameters (Hb, RBCs and WBCs) from anemic values to the normal values. Liposome encapsulation for MNPs increased the bioavailability of iron, enhanced drug biocompatibility and decreased toxicity on parenchymatous organs (Liver, spleen and kidney). Therefore, one would recommend the use of LMNPs as a therapeutic drug for IDA treatment as it showed a success in overcoming the side effects that accompanied the use of traditional drugs.

Declaration of competing interest

The authors declare no conflict of interest.

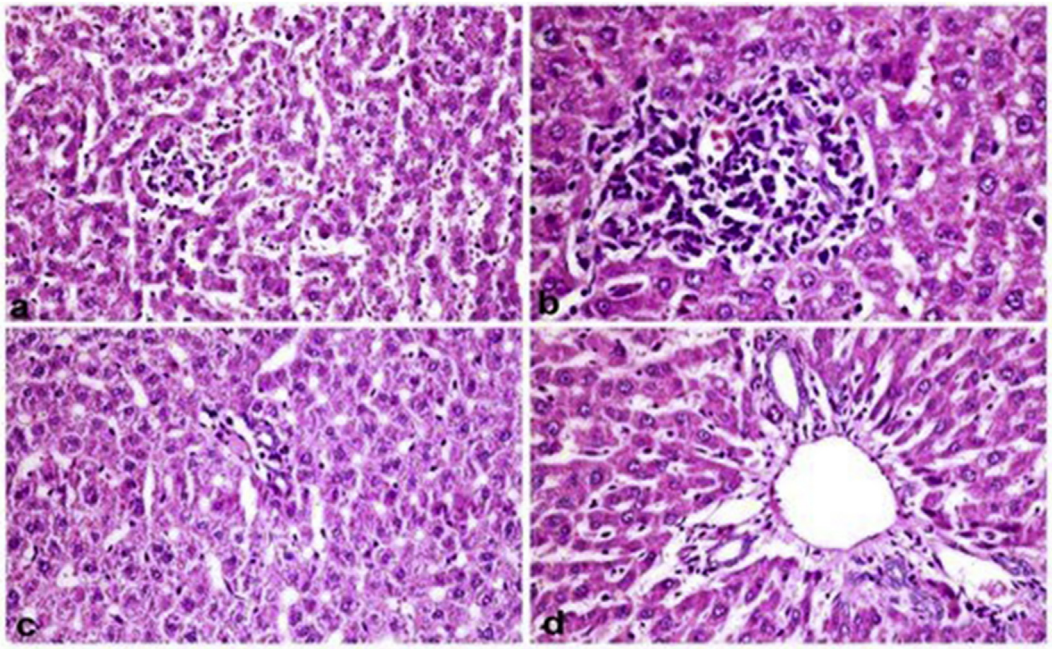

Fig. 6. Histological section of the liver (H&E, X400). (a) +ve control group showing focal hepatocellular necrosis (long arrow) with mononuclear cell aggregation and mild sinusoidal leucocytosis (short arrow). (b) FeSO4-treated group showing mononuclear cell infiltration in portal area (long arrow) with fine hemosiderin pigment deposition in macrophages (short arrow). (c) MNPs- treated group showing scarce mononuclear cell infiltration in small portal area (arrow) with mild Kupffer cell activation. (d) LMNPs -treated group showing normal histological structure of portal area. (Number per group = seven rats). (Scale bar: 50 μm).

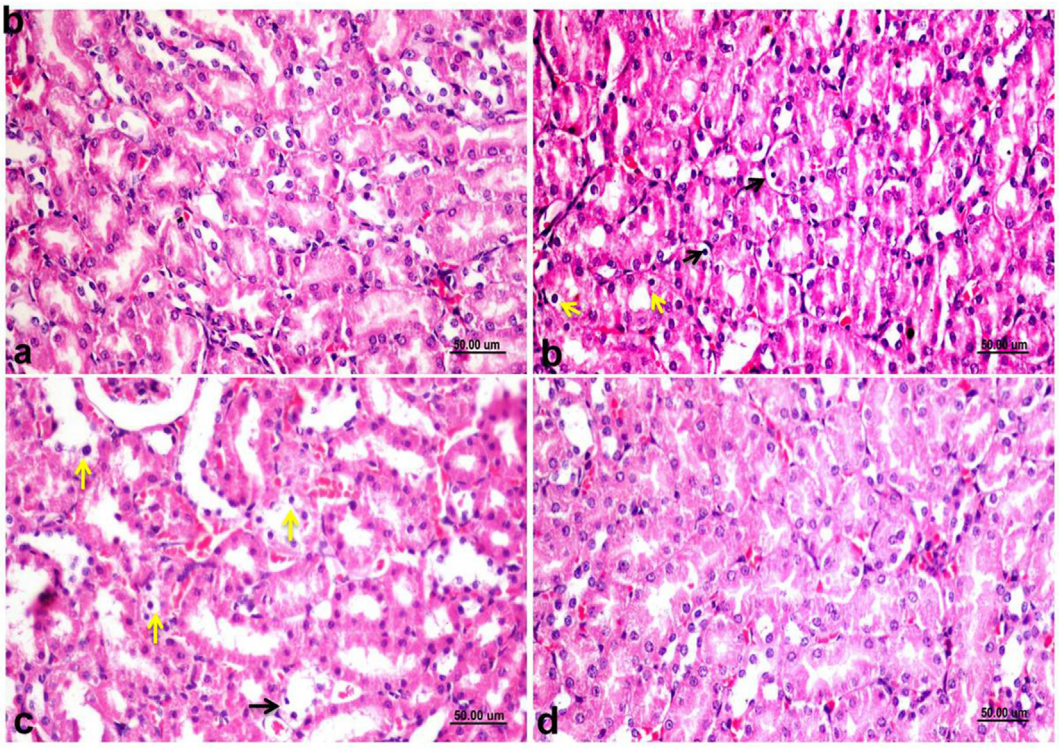

Fig. 7. Histological section of the kidney (H&E, X400). (a) The control untreated group showing normal histological structure of the tubular epithelium. (b) +ve control group showing vacuolization (yellow arrows) and pyknosis of renal tubular epithelial nuclei (black arrow). (c) FeSO4-treated group showing vacuolization (yellow arrows) and pyknosis of individual tubular epithelial nuclei (black arrows). (d) MNPs-treated group showing normal histological structure of renal tubular epithelium. (Number per group = seven rats). (Scale bar: 50 μm). (For interpretation of the references to color in this figure legend, the reader is referred to the web version of this article.)

References

[1] World Health Organization, & UNICEF. UNU, Iron Deficiency Anaemia. Assessment, Prevention and Control. A Guide for Programme Managers, World Health Organization, Geneva, Switzerland, 2001 (Publication WHO/NHD/01.3).

[2] WHO, C, Assessing the Iron Status of Populations: Including Literature Reviews: Report of a Joint World Health Organization, Centers for Disease Control and Prevention Technical Consultation on the Assessment of Iron Status at the Population Level, Geneva, Switzerland, 2004, pp. 6–8.

[3] W. Reinisch, M. Staun, S. Bhandari, M. Muñoz, State of the iron: how to diagnose and efficiently treat iron deficiency anemia in inflammatory bowel disease, J. Crohn's Colitis 7 (6) (2013) 429–440.

[4] A. Shander, L.T. Goodnough, M. Javidroozi, M. Auerbach, J. Carson, W.B. Ershler, ... I. Lew, Iron deficiency anemia—bridging the knowledge and practice gap, Transfus. Med. Rev. 28 (3) (2014) 156–166.

[5] J.L. Miller, Iron deficiency anemia: a common and curable disease, Cold Spring Harbor Perspectives in Medicine 3 (7) (2013) a011866.

[6] F. Oliveira, S. Rocha, R. Fernandes, Iron metabolism: from health to disease, J. Clin. Lab. Anal. 28 (3) (2014) 210–218.

[7] M.M.M. Odeh, Prevalence of Iron Deficiency Anemia among School Children in Salfeet District, Doctoral dissertation An-Najah National University, 2006.

[8] R.J. Stoltzfus, L. Mullany, R.E. Black, Iron Deficiency Anaemia. Comparative Quantification of Health Risks: Global and Regional Burden of Disease Attributable to Selected Major Risk Factors, vol. 1, (2004), pp. 163–209.

[9] A. Khalafallah, A. Dennis, J. Bates, G. Bates, I.K. Robertson, L. Smith, ... J.E.J. Rasko, A prospective randomized, controlled trial of intravenous versus oral iron for moderate iron deficiency anaemia of pregnancy, J. Intern. Med. 268 (3) (2010) 286–295.

[10] Z. Tolkien, L. Stecher, A.P. Mander, D.I. Pereira, J.J. Powell, Ferrous sulfate supplementation causes significant gastrointestinal side-effects in adults: a systematic review and meta-analysis, PLoS One 10 (2) (2015) e0117383.

[11] A.I.D. Souza, M. Batista Filho, C.C. Bresani, L.O.C. Ferreira, J.N. Figueiroa, Adherence and side effects of three ferrous sulfate treatment regimens on anemic pregnant women in clinical trials, Cadernos de Saude Publica 25 (6) (2009) 1225–1233.

[12] M. Zaim, L. Piselli, P. Fioravanti, C. Kanony-Truc, Efficacy and tolerability of a prolonged release ferrous sulphate formulation in iron deficiency anaemia: a non-inferiority controlled trial, Eur. J. Nutr. 51 (2) (2012) 221–229.

[13] D.I. Pereira, S.F. Bruggraber, N. Faria, L.K. Poots, M.A. Tagmount, M.F. Aslam, ... J.J. Powell, Nanoparticulate iron (III) oxo-hydroxide delivers safe iron that is well absorbed and utilised in humans, Nanomedicine 10 (8) (2014) 1877–1886.

[14] M.R. Preiss, E. Cournoyer, K.L. Paquin, E.A. Vuono, K. Belanger, E. Walsh, ... G.D. Bothun, Tuning the multifunctionality of iron oxide nanoparticles using self-assembled mixed lipid layers, Bioconjug. Chem. 28 (11) (2017) 2729–2736.

[15] Y. Shen, L. Posavec, S. Bolisetty, F.M. Hilty, G. Nyström, J. Kohlbrecher, ... R. Mezzenga, Amyloid fibril systems reduce, stabilize and deliver bioavailable nanosized iron, Nat. Nanotechnol. 12 (7) (2017) 642.

[16] E.D.T.A. Salah, M.M. Bakr, H.M. Kamel, K.M. Abdel, Magnetite Nanoparticles as a Single Dose Treatment for Iron Deficiency Anemia, (2010) (Google Patents, WO2010034319A1, 1).

[17] V. Garcés, A. Rodríguez-Nogales, A. González, N. Gálvez, M.E. Rodríguez-Cabezas, M.L. García-Martin, ... J.M. Dominguez-Vera, Bacteria-carried iron oxide nanoparticles for treatment of anemia, Bioconjug. Chem. 29 (5) (2018) 1785–1791.

[18] Mahmoud, M. B. M., & Helmy, S. H. A. (2016). U.S. Patent Application No. 14/772, 648.

[19] M.A. Elshemy, Iron oxide nanoparticles versus ferrous sulfate in treatment of iron deficiency anemia in rats, Egyptian Journal of Veterinary Sciences 49 (2) (2018) 103–109.

[20] Y. Gu, Y. Li, Y. Yang, Q. Luo, Y. Zhang, C. Zhou, One-pot facile fabrication of bioavailable iron nanoparticles with good biocompatibility for anemia therapy, Medical Science Monitor: International Medical Journal of Experimental and Clinical Research 24 (2018) 6449.

[21] J. García-Fernández, J. Bettmer, N. Jakubowski, U. Panne, E. Añón, M. Montes-Bayón, A. Sanz-Medel, The fate of iron nanoparticles used for treatment of iron deficiency in blood using mass-spectrometry based strategies, Microchim. Acta 184 (10) (2017) 3673–3680.

[22] R. Kheiri, M.K. Koohi, G. Sadeghi-Hashjin, H. Nouri, N. Khezli, M.A. Hassan, ... M. Motaghinejad, Comparison of the effects of iron oxide, as a new form of iron supplement, and ferrous sulfate on the blood levels of iron and total iron-binding globulin in the rabbit, Iranian Journal of Medical Sciences 42 (1) (2017) 79.

[23] M. Mahmoudi, S. Sant, B. Wang, S. Laurent, T. Sen, Superparamagnetic iron oxide nanoparticles (SPIONs): development, surface modification and applications in chemotherapy, Adv. Drug Deliv. Rev. 63 (1–2) (2011) 24–46.

[24] M. Arruebo, R. Fernández-Pacheco, M.R. Ibarra, J. Santamaría, Magnetic nanoparticles for drug delivery, Nano Today 2 (3) (2007) 22–32.

[25] S.A. Wahajuddin, Superparamagnetic iron oxide nanoparticles: magnetic nanoplatforms as drug carriers, Int. J. Nanomedicine 7 (2012).

[26] R. Rajeswari, R. Jothilakshmi, Magnetic nanoparticles as drug carriers, Materials Science Forum, vol. 807, Trans Tech Publications, 2015, pp. 1–12.

[27] B. Chaize, J.P. Colletier, M. Winterhalter, D. Fournier, Encapsulation of enzymes in liposomes: high encapsulation efficiency and control of substrate permeability, Artificial Cells, Blood Substitutes, and Biotechnology 32 (1) (2004) 67–75.

[28] R.R Wakaskar, General overview of lipid–polymer hybrid nanoparticles,

dendrimers, micelles, liposomes, spongosomes and cubosomes, Journal of drug targeting 26 (4) (2018) 311–318.
[29] M.R. Faria, M.B.F. Martins, M.C. Gonçalves, Development and Characterization of Magnetoliposomes for Drug Delivery Applications, MasterÂs Degree Dissertation in Biomedical Engineering IST-UTL, 2011.
[30] M.R. Faria, M.M. Cruz, M.C. Gonçalves, A. Carvalho, G. Feio, M.B.F. Martins, Synthesis and characterization of magnetoliposomes for MRI contrast enhancement, Int. J. Pharm. 446 (1–2) (2013) 183–190.
[31] M.M. Mady, M.M. Fathy, T. Youssef, W.M. Khalil, Biophysical characterization of gold nanoparticles-loaded liposomes, PhysicaMedica 28 (4) (2012) 288–295.
[32] E.R. Dadashzadeh, M. Hobson, L. Henry Bryant Jr., D.D. Dean, J.A. Frank, Rapid spectrophotometric technique for quantifying iron in cells labeled with superparamagnetic iron oxide nanoparticles: potential translation to the clinic, Contrast Media & Molecular Imaging 8 (1) (2013) 50–56.
[33] Y. Leng, Materials Characterization: Introduction to Microscopic and Spectroscopic Methods, John Wiley & Sons, 2009.
[34] Instruments, M, Dynamic light scattering: an introduction in 30 minutes, Technical Note Malvern, MRK656-01, 2012, pp. 1–8.
[35] D. Paolino, P. Sinha, M. Fresta, M. Ferrari, Drug delivery systems, Encyclopedia of Medical Devices and Instrumentation, 2006.
[36] X. Wang, Z. Teng, H. Wang, C. Wang, Y. Liu, Y. Tang, ... G. Lu, Increasing the cytotoxicity of doxorubicin in breast cancer MCF-7 cells with multidrug resistance using a mesoporous silica nanoparticle drug delivery system, Int. J. Clin. Exp. Pathol. 7 (4) (2014) 1337.
[37] L. Rieznichenko, A. Doroshenko, T. Gruzina, S. Dybkova, Z. Polova, Z. Ulberg, I. Chekman, Iron Nanoparticles' Effectiveness for New Antianemic Preparations Development, (2013) In Nanocon (P. 556).
[38] R. Chaturvedi, P. Chattopadhyay, S. Banerjee, C.R. Bhattacharjee, P. Raul, K. Borah, ... V. Veer, Iron-rich drinking water and ascorbic acid supplementation improved hemolytic anemia in experimental Wistar rats, Int. J. Food Sci. Nutr. 65 (7) (2014) 856–861.
[39] L. Yang, H. Kuang, W. Zhang, Z.P. Aguilar, Y. Xiong, W. Lai, ... H. Wei, Size dependent biodistribution and toxicokinetics of iron oxide magnetic nanoparticles in mice, Nanoscale 7 (2) (2015) 625–636.
[40] S. Laurent, D. Forge, M. Port, A. Roch, C. Robic, L. Vander Elst, R.N. Muller, Magnetic iron oxide nanoparticles: synthesis, stabilization, vectorization, physicochemical characterizations, and biological applications, Chem. Rev. 108 (6) (2008) 2064–2110.
[41] Y. Chen, B. Chen, Application and development of magnetic ironoxide nanoparticles in tumor-targeted therapy, Ai Zheng 29 (1) (2010) 118–122.
[42] A.J. Cole, A.E. David, J. Wang, C.J. Galbán, V.C. Yang, Magnetic brain tumor targeting and biodistribution of long-circulating PEG-modified, cross-linked starch-coated iron oxide nanoparticles, Biomaterials 32 (26) (2011) 6291–6301.
[43] B.B. Pultrum, E.J. Van der Jagt, H.L. Van Westreenen, H.M. Van Dullemen, P. Kappert, H. Groen, ... G.M. Van Dam, Detection of lymph node metastases with ultrasmall superparamagnetic iron oxide (USPIO)-enhanced magnetic resonance imaging in oesophageal cancer: a feasibility study, Cancer Imaging 9 (1) (2009) 19.
[44] O. Veiseh, C. Sun, C. Fang, N. Bhattarai, J. Gunn, F. Kievit, ... J. Olson, Specific targeting of brain tumors with an optical/magnetic resonance imaging nanoprobe across the blood-brain barrier, Cancer Res. 69 (15) (2009) 6200–6207.
[45] K.C. Briley-Saebo, Y.S. Cho, P.X. Shaw, S.K. Ryu, V. Mani, S. Dickson, ... S. Tsimikas, Targeted iron oxide particles for in vivo magnetic resonance detection of atherosclerotic lesions with antibodies directed to oxidation-specific epitopes, J. Am. Coll. Cardiol. 57 (3) (2011) 337–347.
[46] A. Iannone, R.L. Magin, T. Walczak, M. Federico, H.M. Swartz, A. Tomasi, V. Vannini, Blood clearance of dextran magnetite particles determined by a non-invasive in vivo ESR method, Magn. Reson. Med. 22 (2) (1991) 435–442.
[47] H. Arami, A. Khandhar, D. Liggitt, K.M. Krishnan, In vivo delivery, pharmacokinetics, biodistribution and toxicity of iron oxide nanoparticles, Chem. Soc. Rev. 44 (23) (2015) 8576–8607.
[48] N.B. Shah, G.M. Vercellotti, J.G. White, A. Fegan, C.R. Wagner, J.C. Bischof, Blood–nanoparticle interactions and in vivo biodistribution: impact of surface PEG and ligand properties, Mol. Pharm. 9 (8) (2012) 2146–2155.
[49] T.L. Doane, C.H. Chuang, R.J. Hill, C. Burda, Nanoparticle ζ-potentials, Acc. Chem. Res. 45 (3) (2011) 317–326.
[50] R.R. Arvizo, O.R. Miranda, D.F. Moyano, C.A. Walden, K. Giri, R. Bhattacharya, ... P. Mukherjee, Modulating pharmacokinetics, tumor uptake and biodistribution by engineered nanoparticles, PLoS One 6 (9) (2011) e24374.
[51] K.E. Sapsford, W.R. Algar, L. Berti, K.B. Gemmill, B.J. Casey, E. Oh, ... I.L. Medintz, Functionalizing nanoparticles with biological molecules: developing chemistries that facilitate nanotechnology, Chem. Rev. 113 (3) (2013) 1904–2074.
[52] M. Mahmoudi, S. Sheibani, A.S. Milani, F. Rezaee, M. Gauberti, R. Dinarvand, H. Vali, Crucial role of the protein corona for the specific targeting of nanoparticles, Nanomedicine 10 (2) (2015) 215–226.
[53] M. De Cuyper, S.J. Soenen, Cationic magnetoliposomes, Liposomes, Humana Press, 2010, pp. 97–111.
[54] S. Xia, S. Xu, Ferrous sulfate liposomes: preparation, stability and application in fluid milk, Food Res. Int. 38 (3) (2005) 289–296.
[55] G. Gregoriadis (Ed.), Liposome Technology: Interactions of Liposomes With the Biological Milieu, vol. 3, CRC Press, 2006.
[56] M.I. Papisov, A. Bogdanov Jr., B. Schaffer, N. Nossiff, T. Shen, R. Weissleder, T.J. Brady, Colloidal magnetic resonance contrast agents: effect of particle surface on biodistribution, J. Magn. Magn. Mater. 122 (1–3) (1993) 383–386.
[57] B. Chertok, A.J. Cole, A.E. David, V.C. Yang, Comparison of electron spin resonance spectroscopy and inductively-coupled plasma optical emission spectroscopy for biodistribution analysis of iron-oxide nanoparticles, Mol. Pharm. 7 (2) (2010) 375–385.
[58] K. Xiao, J. Luo, Y. Li, W. Xiao, J.S. Lee, A.M. Gonik, K.S. Lam, The passive targeting of polymeric micelles in various types and sizes of tumor models, Nanosci. Nanotechnol. Lett. 2 (2) (2010) 79–85.
[59] C. Schweiger, R. Hartmann, F. Zhang, W.J. Parak, T.H. Kissel, P. Rivera_Gil, Quantification of the internalization patterns of superparamagnetic iron oxide nanoparticles with opposite charge, Journal of Nanobiotechnology 10 (1) (2012) 28.
[60] U. Sakulkhu, M. Mahmoudi, L. Maurizi, J. Salaklang, H. Hofmann, Protein corona composition of superparamagnetic iron oxide nanoparticles with various physicochemical properties and coatings, Sci. Rep. 4 (2014) 5020.
[61] C. Boyer, M.R. Whittaker, V. Bulmus, J. Liu, T.P. Davis, The design and utility of polymer-stabilized iron-oxide nanoparticles for nanomedicine applications, NPG Asia Materials 2 (1) (2010) 23.
[62] J.P.M. Almeida, A.L. Chen, A. Foster, R. Drezek, In vivo biodistribution of nanoparticles, Nanomedicine 6 (5) (2011) 815–835.
[63] P.P. Karmali, Y. Chao, J.H. Park, M.J. Sailor, E. Ruoslahti, S.C. Esener, D. Simberg, Different effect of hydrogelation on antifouling and circulation properties of dextran–iron oxide nanoparticles, Mol. Pharm. 9 (3) (2012) 539–545.
[64] Y. Duan, J. Liu, L. Ma, N. Li, H. Liu, J. Wang, ... J. Yan, Toxicological characteristics of nanoparticulate anatase titanium dioxide in mice, Biomaterials 31 (5) (2010) 894–899.
[65] Y. Zhang, X. Sun, C. Xie, X. Shu, A.O. Oso, Z. Ruan, ... Y. Yin, Effects of ferrous carbamoyl glycine on iron state and absorption in an iron-deficient rat model, Genes Nutr. 10 (6) (2015) 54.
[66] N. Tang, L.Q. Chen, H. Zhuang, Effects of heme iron enriched peptide on iron deficiency anemia in rats, Food Funct. 5 (2) (2014) 390–399.
[67] J. Gao, W. Zhang, P. Huang, B. Zhang, X. Zhang, B. Xu, Intracellular spatial control of fluorescent magnetic nanoparticles, J. Am. Chem. Soc. 130 (12) (2008) 3710–3711.
[68] F.M. Hilty, A. Teleki, F. Krumeich, R. Büchel, R.F. Hurrell, S.E. Pratsinis, M.B. Zimmermann, Development and optimization of iron-and zinc-containing nanostructured powders for nutritional applications, Nanotechnology 20 (47) (2009) 475101.
[69] I. Grissa, J. Elghoul, L. Ezzi, S. Chakroun, E. Kerkeni, M. Hassine, ... Z. Haouas, Anemia and genotoxicity induced by sub-chronic intragastric treatment of rats with titanium dioxide nanoparticles, Mutation Research/Genetic Toxicology and Environmental Mutagenesis 794 (2015) 25–31.
[70] M. Mahmoudi, M.A. Shokrgozar, A. Simchi, M. Imani, A.S. Milani, P. Stroeve, ... S. Bonakdar, Multiphysics flow modeling and in vitro toxicity of iron oxide nanoparticles coated with poly (vinyl alcohol), J. Phys. Chem. C 113 (6) (2009) 2322–2331.
[71] F.M. Hilty, M. Arnold, M. Hilbe, A. Teleki, J.T. Knijnenburg, F. Ehrensperger, ... M.B. Zimmermann, Iron from nanocompounds containing iron and zinc is highly bioavailable in rats without tissue accumulation, Nat. Nanotechnol. 5 (5) (2010) 374.
[72] P. Guardia, A. Riedinger, H. Kakwere, F. Gazeau, T. Pellegrino, Daniel Ruiz-Molina, Fernando Novio, Claudio Roscini (Eds.), Magnetic Nanoparticles for Magnetic Hyperthermia and Controlled Drug Delivery, 2015.
[73] J.A. Rogers, K.E. Anderson, The potential of liposomes in oral drug delivery, Crit. Rev. Ther. Drug Carrier Syst. 15 (5) (1998).
[74] T. Lian, R.J. Ho, Trends and developments in liposome drug delivery systems, J. Pharm. Sci. 90 (6) (2001) 667–680.
[75] E.H. Shafie, S.A. Keshavarz, M.E. Kefayati, F. Taheri, P. Sarbakhsh, M.R. Vafa, The effects of nanoparticles containing iron on blood and inflammatory markers in comparison to ferrous sulfate in anemic rats, Int. J. Prev. Med. 7 (2016).
[76] J.D. Cook, Diagnosis and management of iron-deficiency anaemia, Best Pract. Res. Clin. Haematol. 18 (2) (2005) 319–332.
[77] P. Santiago, Ferrous versus ferric oral iron formulations for the treatment of iron deficiency: a clinical overview, Sci. World J. 2012 (2012).
[78] J.U. Okebe, D. Yahav, R. Shbita, M. Paul, Oral iron supplements for children in malaria-endemic areas, Cochrane Database Syst. Rev. 10 (2011).
[79] J.P. Peña-Rosas, L.M. De-Regil, F.E. Viteri, Daily oral iron supplementation during pregnancy, The Cochrane Database of Systematic Reviews 12 (2012) CD004736.
[80] M.J. Cancelo-Hidalgo, C. Castelo-Branco, S. Palacios, J. Haya-Palazuelos, M. Ciria-Recasens, J. Manasanch, L. Pérez-Edo, Tolerability of different oral iron supplements: a systematic review, Curr. Med. Res. Opin. 29 (4) (2013) 291–303.
[81] E. Ahn, N. Pairaudeau, Y. Cérat, B. Couturier, A. Fortier, É. Paradis, G. Koren, A randomized cross over trial of tolerability and compliance of a micronutrient supplement with low iron separated from calcium vs high iron combined with calcium in pregnant women [ISRCTN56071145], BMC Pregnancy and Childbirth 6 (1) (2006) 10.
[82] L. Saha, P. Pandhi, S. Gopalan, S. Malhotra, P. kumarSaha, Comparison of efficacy, tolerability, and cost of iron polymaltose complex with ferrous sulphate in the treatment of iron deficiency anemia in pregnant women, Medscape Gen. Med. 9 (1) (2007) 1.
[83] A. Carley, Anemia: when is it iron deficiency? Pediatr. Nurs. 29 (2) (2003) 127.
[84] Q. Feng, Y. Liu, J. Huang, K. Chen, J. Huang, K. Xiao, Uptake, distribution, clearance, and toxicity of iron oxide nanoparticles with different sizes and coatings, Sci. Rep. 8 (1) (2018) 2082.
[85] I. Raynal, P. Prigent, S. Peyramaure, A. Najid, C. Rebuzzi, C. Corot, Macrophage endocytosis of superparamagnetic iron oxide nanoparticles: mechanisms and comparison of ferumoxides and ferumoxtran-10, Investig. Radiol. 39 (1) (2004) 56–63.
[86] W.J. Rogers, P. Basu, Factors regulating macrophage endocytosis of nanoparticles: implications for targeted magnetic resonance plaque imaging, Atherosclerosis 178 (1) (2005) 67–73.

[87] W.T. Al-Jamal, K. Kostarelos, Liposome–Nanoparticle Hybrids for Multimodal Diagnostic and Therapeutic Applications, (2007).
[88] A. Carvalho, M.C. Gonçalves, M.B.F. Martins, D. Meixedo, G. Feio, Relaxivities of magnetoliposomes: the effect of cholesterol, Magn. Reson. Imaging 31 (4) (2013) 610–612.
[89] M. De Cuyper, W. Noppe, Extractability of the phospholipid envelope of magnetoliposomes by organic solvents, J. Colloid Interface Sci. 182 (2) (1996) 478–482.
[90] M.L. Immordino, F. Dosio, L. Cattel, Stealth liposomes: review of the basic science, rationale, and clinical applications, existing and potential, Int. J. Nanomedicine 1 (3) (2006) 297.
[91] S.J. Soenen, U. Himmelreich, N. Nuytten, M. De Cuyper, Cytotoxic effects of iron oxide nanoparticles and implications for safety in cell labelling, Biomaterials 32 (1) (2011) 195–205.
[92] D. Frascione, C. Diwoky, G. Almer, P. Opriessnig, C. Vonach, K. Gradauer, ... R. Prassl, Ultrasmall superparamagnetic iron oxide (USPIO)-based liposomes as magnetic resonance imaging probes, Int. J. Nanomedicine 7 (2012) 2349.
[93] G. Li, L. Cao, Z. Zhou, Z. Chen, Y. Huang, Y. Zhao, Rapamycin loaded magnetic Fe3O4/carboxymethylchitosan nanoparticles as tumor-targeted drug delivery system: synthesis and in vitro characterization, Colloids Surf. B: Biointerfaces 128 (2015) 379–388.
[94] A.A. Gabizon, Applications of liposomal drug delivery systems to cancer therapy, Nanotechnology for Cancer Therapy, CRC Press, 2006, pp. 603–619.
[95] D.B. Fenske, P.R. Cullis, Entrapment of small molecules and nucleic acid–based drugs in liposomes, Methods in Enzymology, vol. 391, Academic Press, 2005, pp. 7–40.
[96] S. Gui, Z. Zhang, L. Zheng, Y. Cui, X. Liu, N. Li, ... J. Cheng, Molecular mechanism of kidney injury of mice caused by exposure to titanium dioxide nanoparticles, J. Hazard. Mater. 195 (2011) 365–370.
[97] I. Bates, B.J. Bain, 23 Approach to the Diagnosis and Classification of Blood Diseases, (2006).
[98] A.T.H. Mossa, M.A. Abbassy, Adverse haematological and biochemical effects of certain, Research Journal of Environmental Toxicology 6 (4) (2012) 160–168.
[99] S. Pande, P.N. Saxena, B. Bhushan, N. Saxena, Peripheral blood and bone marrow responses under stress of cypermethrin in albino rats, Interdiscip. Toxicol. 7 (1) (2014) 33–40.
[100] P.A. Valberg, J.P. Butler, Magnetic particle motions within living cells. Physical theory and techniques, Biophys. J. 52 (4) (1987) 537–550.